ChemComm

Accepted Manuscript

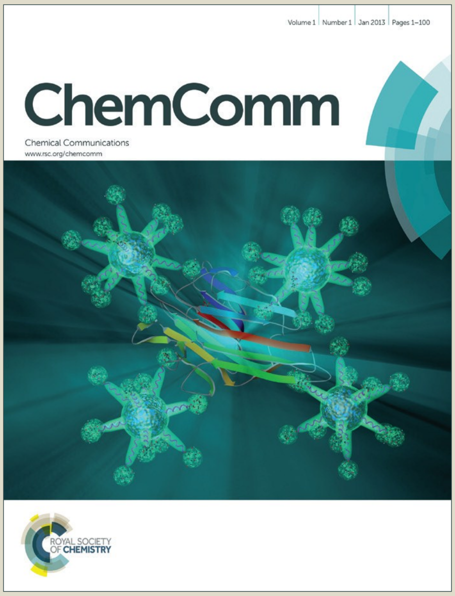

ROYAL SOCIETY
OF CHEMISTRY

www.rsc.org/chemcomm

Chemical Communications

COMMUNICATION

Dynamic configuration of reduced graphene oxide in aqueous dispersion and its effect on thin film properties

Received 00th January 20xx,
Accepted 00th January 20xx

DOI: 10.1039/x0xx00000x

www.rsc.org/

Yufei Wang,[a] Xuahua Zhang[b*] and Dan Li[a]*

Dynamic configuration of reduced graphene oxide (rGO) in aqueous dispersion is revealed by several characterization methods, showing spontaneous and seemingly irreversible configuration transition from flat to highly corrugated sheet over time. Such dynamic behaviour of rGO leads to tailored porous structure of graphene-based thin films. This affects their permeation and electrochemical properties, as well as future industry adoption of graphene.

From a chemistry point of view, graphene can be considered as a giant polymeric molecule with unique two-dimensional configuration.[1] Compared to pristine graphene, reduced graphene oxide (rGO) in aqueous dispersion possesses particular interest due to its cost-effective and large-scalable production[2] as well as the ease of tailoring its configuration,[3] chemistry[4] and intermolecular interactions[5] to allow various new functionalities. As with traditional polymers, utilization of rGO as a molecular building block has enabled the formation of various hierarchical structures, including one-dimensional fibres,[6, 7] two-dimensional membranes[8-10] and three-dimensional foams,[11, 12] for a wide range of potential applications in energy storage,[13, 14] nanofiltration[15, 16] and biomedical areas.[17]

rGO sheets consist of a single layer of sp^2 hybridized carbon atoms with oxygenated functional groups and defects/vacancies.[18] The multiplicity in chemical structure has been suggested to be the origin for the in-plane distortions of freely suspended rGO sheets.[19, 20] Recent research has shown that the corrugated configuration of rGO sheets can be tuned by thermal fluctuation and topological defects, strongly affecting their intrinsic electrical properties as well as the mass transport behaviour of rGO-based thin films.[16] Moreover, such structural features of rGO will also greatly influence its future industry adoption, such as the stability of rGO dispersion during storage and transport.[21] The understanding of the configuration of rGO in aqueous solution is therefore important for both fundamental research and practical utilization of graphene.

A variety of characterization techniques, such as atomic force microscopy (AFM),[2] scanning electron microscopy (SEM),[22] and transmission electron microscopy (TEM)[23] have been used to measure the configuration of graphene sheets. Despite technological difficulty in *in-situ* characterization of their configuration, most of the previous research suggests that their corrugated configuration appears to be static with local strain and distortion facilitating to retain such configuration.[23, 24] In contrast to this general impression, in this work, we report experimental observation of dynamic configuration of rGO sheets in aqueous solution, illustrating a spontaneous and seemingly irreversible configuration transition from rather flat to highly corrugated sheets over time. Such a dynamic behaviour of rGO sheets leads to modified porous structure of graphene-based thin film. This influences their permeation and electrochemical properties, and also shed light on the ability of industrial processing of graphene.

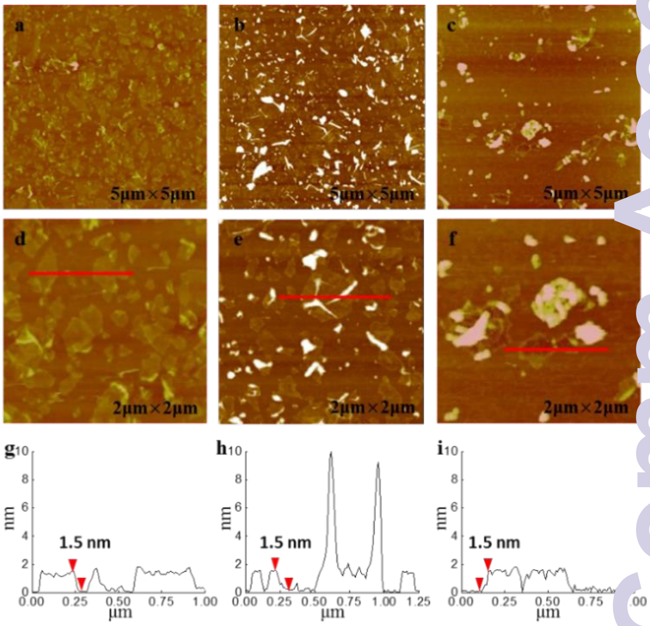

Figure 1 AFM images of rGO sheets on poly-(diallydimeththylammonium chloride) (PDDA) coated mica surface taken in solution in (a, d) stage 1, (b, e) stage 2, and (c, f) stage 3 and (g-i) height profile of the red line in (d-f) respectively.

To directly characterize the conformation of rGO sheets in aqueous dispersion, we have conducted tapping mode AFM measurement in water by following the protocol in our previous report.[16] Typically, the negatively charged rGO sheets were deposited on a positively charged poly(diallyldimethylammonium

---

[a] Department of Materials Science and Engineering, Monash University, VIC 3800, Australia. Email: dan.li2@monash.edu
[b] School of Civil, Environmental and Chemical Engineering, RMIT University, Melbourne, VIC 3001 Australia

Electronic Supplementary Information (ESI) available. DOI: 10.1039/x0xx00000x

chloride (PDDA) coated mica surface in a fluid cell. The electrostatic attractions between rGO sheets and the substrate allow anchoring rGO sheets on the substrate for AFM imaging. Meanwhile, the operation of AFM measurement in liquid state largely maintain the configuration of rGO sheets in aqueous dispersion.[25] As shown in Fig. 1a, the freshly prepared rGO sheets present flat configuration with some random corrugation, and they cover a large portion of the substrate, consistent with our previous observation.[16] Most of the rGO sheets have a lateral size of several tens of nanometres with the height measured to be about 1.5 nm. This value is slightly larger than that reported in the literature (*e.g.* 1 nm),[2, 25, 26] and this is probably due to the presence of water layers between rGO sheets and the substrate.[27]

Remarkably, we found that if the rGO dispersion was held still for certain period of time at room temperature before imaging, the resultant AFM images show configuration change of rGO sheets over time (Fig. 1 and S1-S3). To visualize how the configuration changes with time, we divided the time scale into three stages. In this work, the stage 1 means the freshly prepared rGO dispersion, and stage 2 and 3 represent for 1 week and 2 weeks after the preparation of rGO dispersion, respectively. Note that the rGO dispersion is stable in all 3 stages (Fig S4) without the observation of aggregates. The configuration evolution of rGO sheets in dispersion from mostly flat sheets (*e.g.* in Stage 1) towards more corrugated morphology (*e.g.* in Stage 3) is thus clearly seen in Fig. 1a-1c. More detailed AFM images (Fig. 1d-1f) also reveal this trend where the rGO sheets in dispersion become more and more corrugated over time. Furthermore, some crumpled morphology was observed in stage 3 (Fig. 1c and 1f), indicating the possibility of spontaneous crumpling of rGO sheets in solution. Interestingly, although the observed configuration of rGO sheets changes significantly with time, their thickness remains the same in different stages (Fig. 1g-i). This result suggests that it is the individual rGO sheets that undergo such configuration change, rather than that several rGO sheets aggregate together before depositing onto the solid substrate. In addition, the AFM images also illustrate that the amount of rGO sheets adsorbed on the substrate is significantly reduced from Stage 1 to Stage 3 (Fig. 1a-1f). This is probably because that the configuration evolution of rGO sheets towards more corrugated morphology over time leads to less contact points between rGO sheets and the substrate, which reduces attractive interactions between the negatively-charged functional groups on rGO sheets and the positively-charged substrate. As a result, a decreased coverage of rGO sheets on the substrate is observed, particularly in stage 3 (Fig. 1c and 1f). The AFM images obtained from dried environment also follow the similar trend (Fig S5).

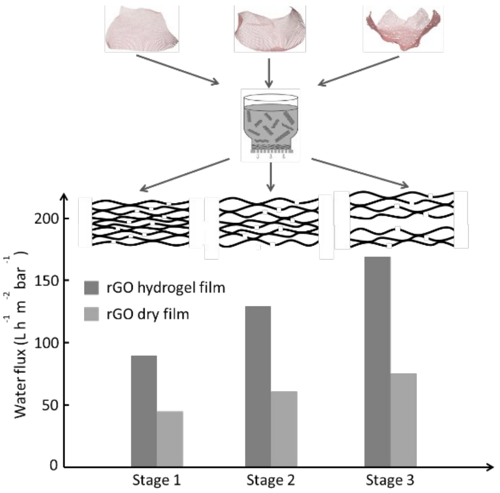

Figure 2 Water permeation of rGO hydrogel and dry films prepared at different stages

To further illustrate the above dynamic behaviour of rGO sheets in aqueous dispersion, we propose the following indirect approaches based on characterizing the porous graphene based thin films. Recent research has shown that rGO sheets can self-assemble in a face-to-face manner, leading to the formation of liquid/gas permeable rGO-based thin films with readily tunable pore size by tailoring the degree of corrugation of rGO sheets.[14, 16] We thus use water molecules and electrolyte ions, respectively, as probes to investigate the porous structure of rGO films so as to reveal the corrugated configuration of individual rGO sheets.

Water permeation experiment was first carried out. According to Hagen-Poiseuille's equation,[28] the water flux generally increases with increase of pore size. Therefore, it is reasonable to assume that the more corrugated rGO sheets will results in a membrane with increased channel size for water molecules to pass through. Indeed, our experimental results based on rGO hydrogel films show an increase of water flux from stage 1 to stage 3 (Fig. 2), indicating more and more corrugated rGO sheets with time, which is consistent with AFM observations. In addition, even if the rGO hydrogel films obtained from different stages are vacuum-dried with reduction of pore size, they present the similar trend (Fig. 2). The above permeation results thus suggest that the configuration transition of rGO sheets with time may be largely irreversible, despite the fact that the applied vacuum pressure tend to flatten the rGO sheets, because otherwise, the similar porous structure of the rGO thin films would exhibit similar permeation performance.

Electrochemical characterizations of vacuum-dried rGO thin films were also conducted to gain an insight into their different porous structures. As demonstrated previously,[29, 30] upon charging-discharging, the electrolyte ions can diffuse into the pores of rGO thin films and adsorb on the surface of rGO sheets to form an electrical double layer (EDL), and this behaviour can be quantified by the calculation of capacitance. Importantly, the dynamic ion adsorption behaviour is highly dependent on the porous structure of the membrane. With the increase of charging-discharging rate, the impedance of ion entering the confined pore space gradually increases, and the ion transport ability becomes to fall behind the shift of the applied potential. This restricts the formation of EDL and will be effectively reflected from the specific capacitance value. In other words, the change of specific capacitance with the increase of charging rate (*i.e.* rate performance) can provide effective means to probe the porous structure of rGO thin films to some extent.[29] Here, dried rGO thin films were prepared using rGO dispersions with the same volume and concentration obtained from Stage 1 to Stage 3, and their thickness was found to be all around 3 μm (Fig. S7). As shown in Fig. 3a, all the rGO thin films exhibit similar capacitance at low charging-discharging rates, indicating similar specific surface area that electrolyte ions can access to. However, with the increase of charging rate, the capacitance variation among all the rGO thin films becomes pronounced. As shown in Fig. 3a and S8, the rate performance of rGO films obtained from Stage1 to Stage 3

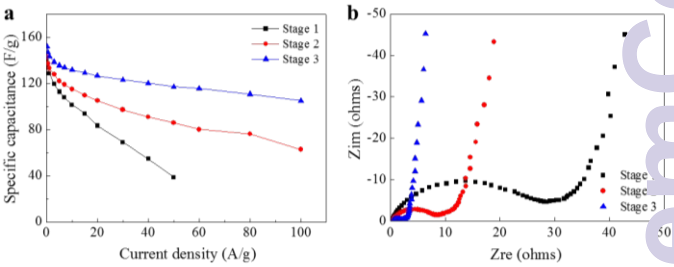

Figure 3 Electrochemical characterizations of vacuum-dried rGO thin films at different time scales: (a) specific capacitance and (b) EIS spectrum

is largely improved, illustrating enhanced ion transport ability. This is also clearly revealed from the Nyquist plot (Fig. 3b) where reduced semi-circle and shortened Warburg-type line from Stage 1 to Stage 3 indicate decreased impedance to ion transport within the porous nanostructure of rGO thin films. These results therefore indicate enlarged pores in dried rGO thin films obtained from Stage 1 to Stage 3, and this is due to the increased degree of corrugation in rGO sheets.

The dynamic configuration of rGO sheets in aqueous solution not only tailors the nanostructure of rGO-based thin films, but also affects further processing of graphene. For example, layer-by-layer technique is a facile method to fabricate graphene-based thin films, and we found that such a thin film can only be successfully formed by using freshly prepared rGO dispersions (Fig. 4a). The non-fresh rGO dispersion (*e.g.* rGO dispersion at Stage 3), however, obtains highly corrugated and even crumpled rGO sheets, leading to less attraction force between rGO sheets and the substrate. This will reduce the amount of rGO sheets anchored to the substrate, limiting the ability to form multi-layered graphene-based films (Fig. 4b).

It is worth noting that previous graphene research mainly focuses on engineering the hierarchical structure of graphene-based materials and improving their performance, but may have overlooked its configuration, likely due to the difficulty of *in-situ* characterization of freely suspended graphene sheets. Our experimental observation of dynamic configuration of rGO clearly suggests its importance on the nanostructure and mass transport properties of graphene-based thin film. Moreover, it is interesting to notice that different rGO configurations are desired for thin-film property improvement and their industry adoption (*e.g.* highly corrugated rGO for capacitive energy storage, and freshly prepared rGO for material processing, respectively). Although we do not fully understand the mechanism of dynamic configuration of rGO sheets in aqueous dispersion at this stage, we found that it is sensitive to the concentration of rGO dispersion (Fig. S6a-b), its chemical structure (Fig. S6c) the presence of additives[2] and the temperature,[16] and the time scale may vary with different batches of rGO. Detailed research will be required to further understand and control of the dynamic configuration of graphene.

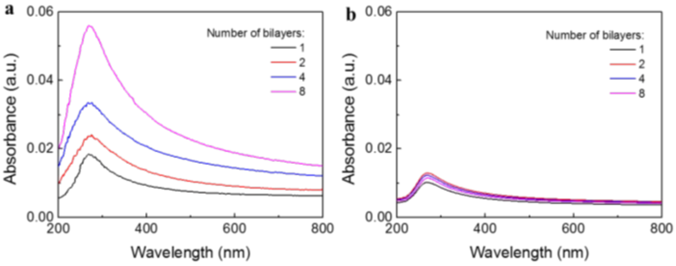

Figure 4 UV-vis spectra of rGO/PDDA films on quartz substrate formed by layer-by-layer deposition using rGO dispersion at (a) Stage 1 and (b) Stage 3.

In conclusion, we report experimental observation of dynamic configuration of rGO sheets in aqueous dispersion which shows spontaneous and seemingly irreversible configuration change over time. The dynamic configuration of rGO sheets leads to varied nanostructure of rGO thin films and their mass transport behaviour. More importantly, such structural features of rGO may raise issues about the stability of rGO dispersion and its nanofabrication when graphene commercialization is considered. This work provides an example illustrating how individual graphene sheets influence the assembly, nanostructure and property of graphene-based macroscopic structures as well as future industrial adoption of graphene.

Acknowledgement

We acknowledge the financial support from the Australian Research Council (FT110100341, DP14012624, and FFT120100473). This work made use of the facilities at the Monash Centre for Electron Microscopy.

Notes and references

1 A. K. Geim, *Science*, 2009, **324**, 1530-1534.

2 D. Li, M. B. Muller, S. Gilje, R. B. Kaner and G. G. Wallace, *Nature Nanotech.*, 2008, **3**, 101-105.

3 A. Fasolino, J. H. Los and M. I. Katsnelson, *Nature Mater.*, 2007, **6**, 858-861.

4 J. Luo, J. Kim and J. Huang, *Acc. Chem. Res.*, 2013, **46**, 2225-2234.

5 Y. Wang, S. Chen, L. Qiu, K. Wang, H. Wang, G. P. Simon and D. Li, *Adv. Funct. Mater.*, 2015, **25**, 126-133.

6 Z. Xu, H. Sun, X. Zhao and C. Gao, *Adv. Mater.*, 2013, **25**, 188-193.

7 G. Huang, C. Hou, Y. Shao, H. Wang, Q. Zhang, Y. Li and M. Zhu, *Sci. Rep.*, 2014, **4**, 4248.

8 L. J. Cote, F. Kim and J. X. Huang, *J. Am. Chem. Soc.*, 2009, **131**, 1043-1049.

9 Y. X. Xu, H. Bai, G. W. Lu, C. Li and G. Q. Shi, *J. Am. Chem. Soc.*, 2008, **130**, 5856-7.

10 X. Yang, L. Qiu, C. Cheng, Y. Wu, Z.-F. Ma and D. Li, *Angew. Chem. Int. Ed.*, 2011, **50**, 7325-7328.

11 L. Qiu, J. Z. Liu, S. L. Y. Chang, Y. Wu and D. Li, *Nature Commun*, 2012, **3**, 1241.

12 Z. Niu, J. Chen, H. H. Hng, J. Ma and X. Chen, *Adv. Mater.*, 2012, **24**, 4144-4150.

13 M. F. El-Kady, V. Strong, S. Dubin and R. B. Kaner, *Science*, 2012, **335**, 1326-1330.

14 X. Yang, C. Cheng, Y. Wang, L. Qiu and D. Li, *Science*, 2013, **341**, 534-537.

15 R. R. Nair, H. A. Wu, P. N. Jayaram, I. V. Grigorieva and A. K. Geim, *Science*, 2012, **335**, 442-444.

16 L. Qiu, X. Zhang, W. Yang, Y. Wang, G. P. Simon and D. Li, *Chem Commun*, 2011, **47**, 5810-5812.

17 T. Sun, G. Qing, B. Su and L. Jiang, *Chem. Soc. Rev.*, 2011, **40**, 2909-2921.

18 K. P. Loh, Q. Bao, P. K. Ang and J. Yang, *J. Mater. Chem.*, 2010, **20**, 2277.

19 C. Gómez-Navarro, J. C. Meyer, R. S. Sundaram, A. Chuvilin, S. Kurasch, M. Burghard, K. Kern and U. Kaiser, *Nano Lett.*, 2010, **10**, 1144-1148.

20 A. Bagri, C. Mattevi, M. Acik, Y. J. Chabal, M. Chhowalla and V. B. Shenoy, *Nature Chem*, 2010, **2**, 581-587.

21 A. Zurutuza and C. Marinelli, *Nature Nanotech.*, 2014, **9**, 730-734.

22 Y. Zhang, J. P. Small, W. V. Pontius and P. Kim, *Appl. Phys. Lett.*, 2005, **86**, 073104.

23 J. C. Meyer, A. K. Geim, M. I. Katsnelson, K. S. Novoselov, T. J. Booth and S. Roth, *Nature*, 2007, **446**, 60-63.

24 N. R. Wilson, P. A. Pandey, R. Beanland, J. P. Rourke, U. Lupo, G. Rowlands and R. A. Römer, *New J. Phys.*, 2010, **12**, 125010.

25 X. Zhang, Y. Wang, S. Watanabe, M. H. Uddin and D. Li, *Soft Matter*, 2011, **7**, 8745-8748.

26 Y. Wang, Y. Song, S. Watanabe, S. Zhang, D. Li and X. Zhang, *ACS Appl. Mater. Interfaces*, 2012, **4**, 6443-6449.

27 K. Xu, P. Cao and J. R. Heath, *Science*, 2010, **329**, 1188-1191.

28 R. W. Baker, Wiley, *Membrane Technology and Applications*, 2nd ed, 2004.

29 C. Cheng, J. Zhu, X. Yang, L. Qiu, Y. Wang and D. Li, *J. Mater. Chem. A*, 2013, **1**, 9332-9340.

30 J. Zhu, C. Cheng, X. Yang, Y. Wang, L. Qiu and D. Li, *Chem. Eur. J.*, 2013, **19**, 3082-3089.

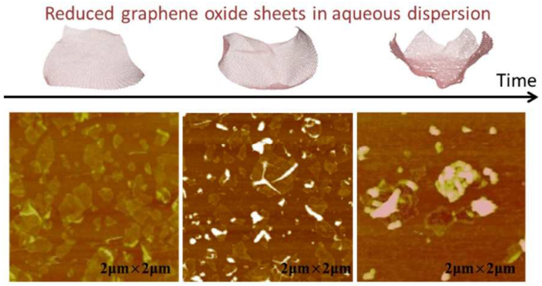

The configuration of reduced graphene oxide sheets in aqueous dispersion is found to be dynamic, showing a remarkable impact on their thin film properties.